First Implementation of the WRF-CHIMERE-EDGAR Modeling System Over Argentina

María Fernanda García Ferreyra, Gabriele Curci, and Mario Lanfri

***Abstract*—Air quality monitoring and research have been gaining importance in Argentina and Latin America, mainly in megacities where pollution reaches critical levels as in other places of the world. This work is a first attempt at simulating pollution levels at the country scale, in order to support air quality management and forecasting activities. We implemented the global scale inventory of anthropogenic emissions EDGAR v4.2 into the CHIMERE chemistry-transport model, driven by WRF meteorological fields, at a resolution of about 50 km, a performance evaluation of the modeling system is presented by the use of ground-based and satellite data. The lack of monitoring stations in the country constrained the evaluation to the March–May 2009 time period in three cities. We obtain a generally large underestimation of nitrogen oxides and particulate matter, but a good simulation of the daily cycles. The magnitude of pollution levels is underestimated probably because of the misrepresentation of the monitoring stations (sites heavily affected by local traffic) and of the coarse resolution of the model. Nitrogen dioxide tropospheric column obtained by the OMI sensor (onboard Aura/NASA) was used to evaluate spatial correspondence with the simulation outputs, revealing that spatial features are broadly captured by the model. Further work would imply an emission inventory refinement and the use of other satellite data available considering other periods of time; however, a more dense and representative air quality monitoring network throughout the country is very much needed.**

***Index Terms*—Air pollution, atmospheric measurements, modeling, remote sensing.**

I. Introduction

ACTIVITIES and research on air pollution have been gaining importance in the main cities of Argentina. Air quality studies in Buenos Aires show similarities with other polluted places in the world with critical levels of NO_x and particulate matter. Along with these results, local environmental agencies have started continuous monitoring activities of criteria pollutants in some of the most populated cities, where industries and population concentrate (see Fig. 1).

Anthropogenic emission inventories in Argentina were elaborated in the areas of Buenos Aires, Bahía Blanca, and Mendoza allowing the development of local air quality modeling. An emission inventory for 1A IPCC sector (fossil fuel burning activities) was estimated for the whole country, though data are not spatially gridded and thus not ready for implementation into air quality models.

Fig. 1. Location of mentioned Argentinian cities.

This work presents the first implementations of a chemical transport model over the entire territory of Argentina. It is made by implementing the global scale inventory of anthropogenic emissions EDGAR v4.2 into the CHIMERE chemistry-transport model [1]. Simulations at $0.5^\circ \times 0.5^\circ$ resolution at country scale were carried out for the period March-May 2009. Performance of the modeling system was evaluated using ground-based and satellite data. The implementation made is of great significance, representing a starting point for future air quality operational forecast and pollutants satellite monitoring in the country.

Manuscript received February 26, 2016; revised May 27, 2016; accepted June 20, 2016. This work presents the first implementations of a chemical transport model over the entire territory of Argentina. *(Corresponding author: María Fernanda García Ferreyra.)*

M. F. García Ferreyra and M. Lanfri are with CONAE, 5187 Falda del Canete, Argentina (e-mail: fgarciaferreyra@conae.gov.ar; lamfri@conae.gov.ar).

G. Curci is with CETEMPS, University of L'Aquila, 67100 L'Aquila, Italy, he is also with the Department of Physical and Chemical Sciences, University of L'Aquila, L'Aquila, Italy (e-mail: gabriele.curci@aquila.infn.it).

Color versions of one or more of the figures in this paper are available online at http://ieeexplore.ieee.org.

Digital Object Identifier 10.1109/JSTARS.2016.2588502

This paper is organized as follows. Section II presents the main Argentinian air quality characteristics. Section III illustrates the WRF-CHIMERE meteorological and chemistry-transport modeling system and presents the implementation of the EDGAR inventory into the modeling system and its comparison with a national inventory. Section IV analyzes the simulation outputs in comparison to available ground and satellite measurements. The final section draws conclusions and future directions.

II. Air Quality in Argentina

The study area defined is the Argentinian continental territory. Argentina extends from latitude $-21.76°$ to $-55.05°$ and longitude from $-53.63°$ to $-73.56°$. Its mainland surface covers 2,791,810 km^2. This vast extension provides the country with a variety of geographical regions characterized by different topographies and climates. To the Center-East, the terrain is plain, and it features a humid climate toward the East; this region concentrates most of the population, and it is where agriculture and livestock are mostly developed. To the South, the Patagonic plateau goes from the Andes to the Atlantic Ocean; weather is usually dry cold and winds are strong. To the West, the topography is defined by the Andes, where the highest mountains are located; these block humidity coming from the Pacific Ocean. To the North and North-East, there are the Chaco and Mesopotamia regions and wooded and selvatic regions, where the climate is subtropical and very humid.

The Metropolitan Area of Buenos Aires (MABA), a megacity of 12.8 million inhabitants, has been the main subject of studies involving emission inventories, dispersion modeling, field campaigns, the study of mixing heights, and the observation and analysis of aerosol optical depths (AOD). The highest levels of primary pollutants were reported near the main railway stations, where background CO may reach values close to 4 ppm and background NO_x may be approximately 400 $\mu\mathrm{g}\cdot\mathrm{m}^{-3}$ [2]. The main source of CO, NO_x, and PM2.5 is traffic [3], but for PM2.5, other sources, such as erosion/resuspension by winds, are also considered important [4]. Summer average daily maximum O_3 1-h concentrations in the MABA vary between 15 ppb in the most densely urbanized areas to 53 ppb in the suburbs (50–60 km downwind downtown) [5]. Particulate material shows higher levels during summer (mean values of about 41 for PM2.5 and 52 $\mu\mathrm{g}\cdot\mathrm{m}^{-3}$ for PM10), though in winter these levels are still high (33 and 44 $\mu\mathrm{g}\cdot\mathrm{m}^{-3}$ for PM2.5 and PM10, respectively). Usually, air pollutants in this area do not accumulate because of its flat topography and high wind speed, though when the wind decreases enough, high levels of pollutants can be observed [3]. The highest hourly daytime mean values of mixing height derived for summer and winter are, respectively, 1170 and 592 m [6]. Often, the concentration levels of PM2.5 are close to, or higher than, the US-EPA alarm value [4]. Several environmental health indicators for air pollution present Buenos Aires as one of the worst cities in Latin America, according to PM10 exposure levels [7].

Córdoba, the second largest city in Argentina (1.3 million inhabitants), is surrounded by hills causing radiative inversion during winter which traps air pollutants in a 200-m-thick layer above surface [8]. Remarkably, 85% of the total emissions are generated by mobile sources which seriously affect the downtown area, characterized by high traffic density [8]. Likewise, on the basis of studies about aerosol elemental composition, it was found that traffic and road/construction dust were the most important sources of particulate material. More than 66% of the composition of PM10 (average 107 $\mu\mathrm{g}\cdot\mathrm{m}^{-3}$) is in the PM2.5 size range [9]. The monitoring of primary pollutants reveals frequent overpasses of local air quality standards. Ozone level is very low within the city due to the high NO levels emitted by mobile sources, though there is ozone formation downwind that can affect neighboring cities [10]. Critical levels of heavy metals were found through biomonitoring techniques [11] and the genotoxicity of particulate material confirmed potential chronic effects of air pollution on human health [12].

Rosario, a city of 1.2 million inhabitants, lays on the coast of Parana river, a very important navigation course. Its climate is warm and humid, with predominant south winds of about 10 $\mathrm{km}\cdot\mathrm{h}^{-1}$. This area is characterized by very frequent rains, rising up to 1040 mm in a year. The closeness of the city to the river and its distribution along the coast allows for a good capacity for removing air pollutants. Since 1994, passive monitoring of nitrogen oxides has been carried out. Traffic has been identified as the most important source of emissions, mostly from private vehicles and public transport (Andres D. A., personal communication in 2013). The city center is characterized by the presence of high buildings that hinder the pollutants dispersion. The NO_2 concentration varies from more than 100 $\mu\mathrm{g}\cdot\mathrm{m}^{-3}$ in winter to less than 80 $\mu\mathrm{g}\cdot\mathrm{m}^{-3}$ in summer (Andres D. A., personal communication in 2013) and its annual mean is within the limits established by local legislation.

Mendoza metropolitan area (850 000 inhabitants) is adjacent to the Andes mountain range which strongly influences local meteorology and, therefore, air quality. The climate is semiarid with high temperatures in summer and very low temperatures in winter. Local rains barely reach 250 mm yearly. Although the high Zonda wind is typical of this region, the average wind speed per year is only 4.2 $\mathrm{km}\cdot\mathrm{h}^{-1}$. Intensive and intermediate industrial activities, along with downtown traffic emissions and residential sources, affect air quality [13]. Regional and meteorological studies on Zonda in the area of Mendoza using numerical weather model has also been presented by Norte, Ulke, Simonelli, and Viale [14] and Puliafito, Allende, Mulena, Cremades, and Lakkis [15]. During summer, the mountain–valley circulation ventilates the city, whereas stagnation often occurs in winter, producing the highest levels of ozone (in the winter of 1996, ozone levels reached 120 $\mu\mathrm{g}\cdot\mathrm{m}^{-3}$ [16]. Previous studies involved the construction of an emission inventory and its implementation into a dispersion and a chemical transport model [17], [18]. Instead, at Malargue (300 km south of the Mendoza city), backward trajectories of aerosols indicated that winter nights with low aerosol concentrations show air masses originating from the Pacific Ocean, and aerosol peaks occurring in September and October could be interpreted as air mass transported from biomass burning in Northern South America [19].

The biggest oil refineries and petrochemical poles in the country are located in La Plata and Bahía Blanca port cities. La Plata also has a very high population density and the highest automobile/person ratio in Argentina (1:2). During autumn and winter, weather conditions in La Plata produce thermal inversions, decreasing pollutants dispersion in the atmosphere [20]. The petrochemical pole in La Plata displays enhanced AOD levels. Daily PM10 values exceeded local air quality standards (150-$\mu g \cdot m^{-3}$ 24-h average, Dec. Reg. 3395, 1996) in 2010. SO_2 levels never surpassed local standards (140 ppb 24-h average); however, SO_2 measurements exceeded the 2005 WHO standard values (8 ppb 24-h average) during all the period under study [20]. Traffic was identified as the main source of VOCs, with levels similar to those reported for other major cities worldwide [21]. Different studies correlate VOCs, PM10, and PAHs (poliaromatic hidrocarbons) high concentrations with effects on health [21]–[23]. The petrochemical pole in Bahía Blanca displays the highest levels of NO_x, SO_2, and NH_3, whereas CO is mainly emitted within the city, and PM10 is influenced by all relevant sources (industries, traffic, and soil erosion). Although the site is heavily industrialized, the impact of those emissions on air quality was found to be less important than transport emissions, because the high-stack point sources disperse much more efficiently [24].

In Tucuman province, there is also intense pollution of the air caused by fires during winter (dry season), in the sugar cane crop area, causing visibility problems and incidence on respiratory diseases [25]–[27]. A biomass burning emission inventory was elaborated for this area [28]. High values of pollutants were found, mainly for CO and particulate matter [28].

In Argentina, a very important source of atmospheric pollutants is anthropogenic and natural biomass burning that contributes to regional and global atmospheric aerosols. In the studies of the continental aerosol load in terms of AOD using satellite observation along with forward trajectory modeling, Castro-Videla, Barnaba, Angelini, Cremades, and Gobbi [29] found that most of the fires produced in the North of Argentina (Chaco forest) occur in July, whereas in the Center-East Pampa region, they peak springtime. The same authors reported that the main human driver of fires is the expansion of soybean crops and sugar cane harvest.

III. Implementation of the Modeling System

CHIMERE [1], an Eulerian multiscale chemical transport model, developed to produce daily forecast for criteria pollutants, to make long-term simulations for emission control scenarios and to study particular cases related to air quality, was implemented in this study to estimate atmospheric pollutant concentrations in Argentina.

The model input data were both the EDGAR global anthropogenic emission database [30] and meteorological information from the WRF [31] numerical weather model; the model is offline regarding meteorological fields. Chemical boundary conditions are taken from the global 3-D chemistry-climate model LMDz-INCA [32] and aerosol boundary conditions from both GOCART [33] and LMDz-AERO [34]–[36] global models. Also, the nine-landuse-class raster was provided by the Global Land Cover Facility [37]. Instead, biogenic emissions are taken from the MEGAN model [38].

The defined spatial domain for air quality mapping includes the continental Argentinian territory. Whereas the horizontal resolution of EDGAR was of $0.1° \times 0.1°$, CHIMERE was configured to have $0.5° \times 0.5°$ horizontal resolution and eight vertical levels until 500-hPa pressure level within the troposphere. Both CHIMERE and WRF use hydrostatic pressure in vertical terrain following coordinates.

In agreement with the availability of the continuous chemical monitoring data, which in Argentina is extremely scarce, the study was defined from March 1 to May 31, in 2009. This time period allowed to have more data in more than one location at the same time. No important forest fires in the region occurred during the period. CHIMERE simulations were performed for 48 h, whereas WRF was run during 54 h, starting 6 h before the CHIMERE running. For both models, hourly results were defined.

WRF is a numerical weather prediction model used to generate hourly meteorological data within the study domain. The NCEP FNL [39] provides the 6-h initial and boundary conditions for the meteorological simulations and USGS is referred to the landuse information. WRF cells are set to have a Lambert conformational geographical projection and an horizontal resolution of 30 × 30 km and 28 vertical levels until it reaches a pressure of 50 hPa. The configuration used for WRF simulations in this study is shown in Table I.

NO_x, CO, NH_3, SO_2, VOCs, and PM10 global emissions estimated for year 2008 in the EDGAR inventory, georeferenced in a horizontal resolution grid of $0.1° \times 0.1°$, are the species used in this work. They contain information by country and are categorized following the IPCC production sectors and subsectors.

Assessing the sensitivity to different combinations of modeling parameterization was outside the scope of this first work. The model setup was done following previous applications of CHIMERE and WRF (e.g., [40] and [41], respectively). Main parameterization used in the modeling system is summarized in Table I.

Whereas CHIMERE is prepared to receive WRF outputs and MOZART2 and GLCF data, this is the first time the EDGAR inventory is used outside the European domain, being needed to develop an EDGAR-CHIMERE interface. To generate the input emission data for CHIMERE, it was necessary to modify the emiSURF v2011 preprocessor, distributed along with CHIMERE. This program is an interface that takes anthropogenic emission inventories in order to generate files with the specific structure needed by CHIMERE, by interpolating the data horizontally and vertically, by disaggregating VOCs and NO_x into real compounds using a speciation profile [42], and by temporarily distributing the SNAP sector species into monthly, daily, and hourly basis. It should be considered that punctual emission sources are simply added to area sources in the current simulation. A specific treatment for point sources

This article has been accepted for inclusion in a future issue of this journal. Content is final as presented, with the exception of pagination.

TABLE I
CHEMICAL AND PHYSICAL OPTIONS FOR THE MODELLING SYSTEM CONFIGURATION

Parameter	CHIMERE options
Version	2011b
INPUT DATA	
Emission inventory	EDGAR v4.2
Meteorological database	WRF
Chemical boundary conditions	MOZART2
Landuse	GLCF
CONFIGURATION PARAMETERS	
Chemistry mechanism	Melchior reduced
Chemically-active aerosols	Yes
Number of aerosol size sections	9
Secondary organic aerosol scheme	Medium scheme
Horizontal resolution	$0.5 \times 0.5^{\circ}$
Vertical resolution	8 levels until 5.5 km
Parameter	WRF options
Version	3.2
Microphysics	WSM3
Longwave radiation	RRTM
Shortwave radiation	Dudhia
Surface layer	Monin-Obukhov
Land surface	Noah LSM
Planetary boundary layer	YSU
Cumulus parameterization	Kain-Fritsch
Horizontal resolution	30 x 30 km
Vertical resolution	28 levels until 20 km
Parameter	EDGAR options
Version	4.2 (2008)
Species	CO, NH_3, NMVOCs, NO_x, SO_2 and PM10
Horizontal resolution	$0.1 \times 0.1^{\circ}$

TABLE II
IPCC TO SNAP SOURCE-SECTOR CONVERSION

IPCC	SNAP	Source-sector
1A1a 1A1bc	SNAP 1	Combustion in energy and transformation industries
1A4	SNAP 2	Nonindustrial combustion (residential, commercial, other)
1A2	SNAP 3	Combustion in manufacturing industry
2A1 2A2 2A7 2B 2C 2D 2E	SNAP 4	Production processes
1B1 1B2 7A 7B 7C 7D	SNAP 5	Extraction/distribution of fossil fuels and geothermal energy
2F1 2F2 2F3 2F4 2G 2F5 3A 3B 3C 3D	SNAP 6	Solvents and other product use
1A3b	SNAP 7	Road transport
1A3a 1A3c 1A3d 1A3e	SNAP 8	Other mobile sources and machinery
6A 6B 6C 6D	SNAP 9	Waste treatment and disposal
4A 4B 4C 4D1 4D2 4D3 4D4 4F 5D	SNAP 10	Agriculture
-	SNAP 11	Biogenic emissions

(e.g., plume rise and dispersion) is not available at the moment in the CHIMERE modeling system.

The steps to build the interface are the following:

1) Download EDGAR database (http://edgar.jrc.ec.europa.eu/). The annual gridded emissions are organized in files by compounds and IPCC sectors, in ton$/0.1^{\circ} \times 0.1^{\circ}$ per year units and ASCII format. Also the annual emissions must be downloaded by country and sector and organized by compound, in CSV format.
2) Emission conversion from IPCC to SNAP 97 production sectors (see Table II).
3) Generation of the data grid. The new emissions are merged from an IPCC sectors separation into a single species file.
4) Definition of a domain in the domainlist file.
5) emiSURF emission interface modification.
6) Compilation of the emiSURF script.

Finally, new files are generated to use the EDGAR emission inventory directly into the CHIMERE model, within the desired domain. These files were successfully tested in CHIMERE v2011b and v2013b.

A. Emission Inventory Overview

Fig. 2 shows how the six compounds introduced by EDGAR split in the SNAP sectors by the emission inventory. It can be seen that Buenos Aires has emissions from a very well characterized city, where NO_x, NH_3, NMVOC, CO, and PM10 come from road transport, SO_x mainly comes from combustion industries, and residential and commercial combustion generates mainly SO_x and PM10 emissions. Córdoba and Bahía Blanca show differences from Buenos Aires emission distribution into the SNAP sectors and amount emitted. On one hand, Córdoba has similarities to an urban area but also shows large incomes from agriculture (NH_3 and PM10), this being different from the PM10 source characterization made in previous studies presented in Section II [9]. The amount of pollutants emitted to the atmosphere is from four to seven times lower than Buenos Aires. Bahía Blanca by EDGAR, on the other hand, does not show any urban or port behavior. Instead, the zone is characterized by agriculture for all the compounds but NO_x and SO_x, being the latter risen by residential and commercial combustion. The amount of pollutants emitted in Bahía Blanca is from 200 to 6×10^{-3} times lower than Buenos Aires, except for PM10 that is only 25 times lower.

In addition, in Fig. 3, the emissions at the three monitoring sites (NO, NO_2, SO_2, CO, and PM10) for a working day, hourly distributed by the emiSURF program, are shown. From the figure, estimated emissions for Córdoba and Bahía Blanca are much lower than in Buenos Aires, except for PM10 which is at the same order of magnitude for the three sites. Moreover, the total of the emissions show an hourly distribution corresponding substantially to road transport, but for PM10 in Córdoba and Bahía Blanca, it is according to the presence agriculture source estimated by EDGAR (see Fig. 2). Every hourly profile comparison, though not for PM10, was made multiplying Córdoba and Bahía Blanca estimated emissions by 10 and 100, respectively.

The EDGAR database was contrasted against a national nongeoreferenced estimation of emissions [43] for year 2000 and IPCC sector 1 (split into 1A, 1B, and 1C sectors). This inventory was built to analyze the evolution of the energetic sector from the national energetic budget. In Fig. 4, the difference between the total amount of the emissions of both inventories can be seen. Sector 1A is referred, on the one hand, to fossil fuel burning by

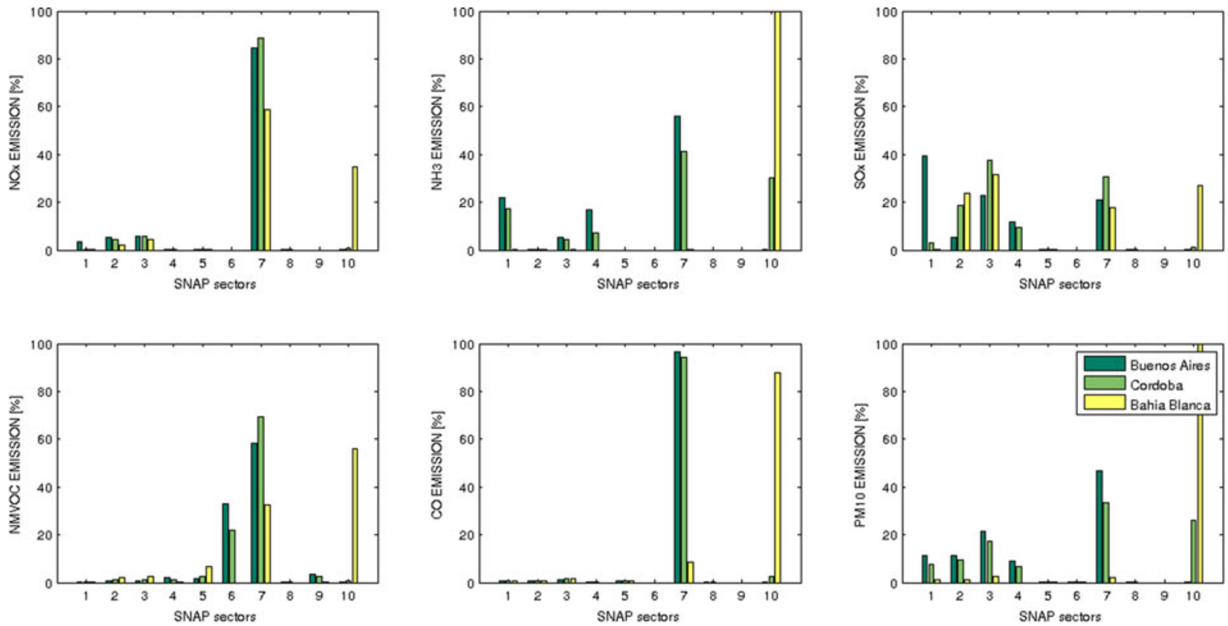

Fig. 2. Percent contribution of SNAP sectors to primary anthropogenic emissions in three Argentinian cities, for which ground-based monitoring stations are available. Annual total emission fluxes are taken from EDGAR v4.2 inventory

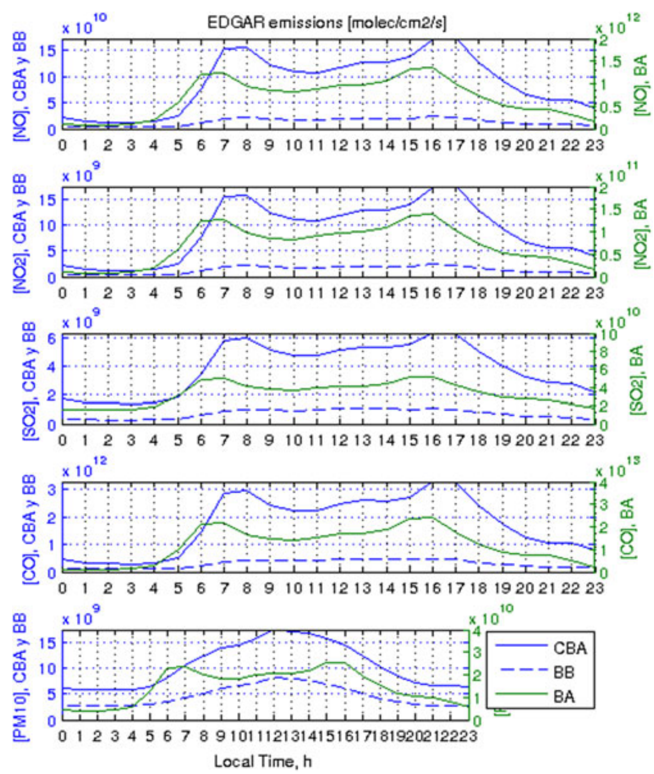

Fig. 3. Daily cycle of anthropogenic emissions estimated by EDGAR v4.2 for the NO, NO_2, SO_2, CO, and PM10 species, for the three monitoring stations. Note that all the emissions in Crdoba and Baha Blanca (exceptPM10) were multiplied by a factor of 10 and 100 respectively, for a better visualization of the emission at an hourly profile.

point sources as energy and manufacturing industries; residential, commercial, and public and agriculture sector emissions, and, on the other hand, by mobile sources as road transport and

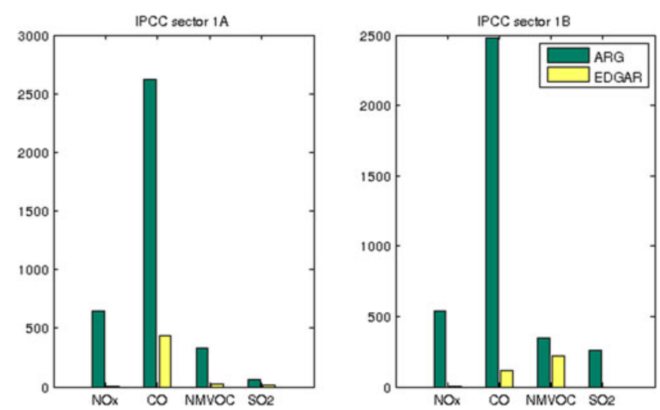

Fig. 4. Comparison between the Argentinian and EDGAR emission inventories, for 1A, 1B, and 1C IPCC sectors.

domestic aviation and navigation. Sector 1B refers to fugitive emissions due to the productive processes around mineral carbon, petroleum, and natural gas obtention. Instead, sector 1C refers to emissions from the international transport (aviation and navigation). The main differences for sector 1A IPCC are that EDGAR considers 17% less than the NO_x estimated emissions by the Argentine inventory and that EDGAR estimated emissions for SO_2 overpass threefold the Argentine inventory estimations. Instead, for sector 1B, IPCC EDGAR estimates only the 25% of the NO_x and CO emissions reported in the Argentinian database and also estimates VOCs nine times higher than the later inventory. For the 1C IPCC sector, EDGAR does not estimate emissions in Argentina for NO_x, CO, VOCs, and SO_2, though for the Argentine inventory they represent 7.3%, 0.3%, 1.2%, and 5.7% respectively, of their sector total.

Along with these results, which indicate the need of reviewing the EDGAR inventory as an input data for the CHIMERE model,

This article has been accepted for inclusion in a future issue of this journal. Content is final as presented, with the exception of pagination.

the work presented by Puliafito, Allende, Pinto, and Castesana [44] discusses the poor geographical distribution of EDGAR inventory for SNAP07 category in Argentina.

IV. Evaluation of the Model System

Air quality models are often evaluated generating deviation statistics between the model predictions and observations, whereas their magnitudes are compared using statistical indexes. This methodology was named as Operational Evaluation, by Dennis *et al.* [45].

Some of the most used indexes for this evaluation type are used in this study: bias, normalized mean bias (NMB), root-mean-square error (RMSE), and correlation coefficient (R), defined by Thunis, Pederzoli, and Pernigotti [46].

Due to the lack of measured data in space and time, the evaluation is not able to solve the incommensurability problem [47], where a punctual measurement and 3-D chemical transport model outputs are different because the last one represents volume-averaged variables.

A. Available Datasets for Model Evaluation

The performance and precision of the modeling system were evaluated by comparing its meteorological and chemical outputs with ground hourly based measurements. The evaluation was performed in three cities—Buenos Aires, Córdoba, and Bahía Blanca—during the simulation period. The air quality monitoring station in Buenos Aires was located in Parque Centenario, a residential–commercial area with medium vehicular flow and few point sources of pollutants. The meteorological station was placed at Aeroparque Metropolitano Jorge Newbery airport, 5 km away from the air quality station, on the coast of Rio de la Plata. In Córdoba, the air quality station was placed in the city center, an area with high vehicular flow. The traffic emissions downtown had an hourly profile related to work and leisure activities. The meteorological station was placed in the city airport, 12 km away from the city center. The third place for evaluation was Bahía Blanca. The monitoring station was located in Ingeniero White, where the petrochemical pole and port are located. The meteorological station, as in the previous cities, was located in the local airport, 12 km away from the air quality station. There were no air quality ground-based measurements that could represent areas with low anthropogenic emissions. For this reason, the comparison to simulations in background scenarios was not possible. The following public institutions provided their measurements to this work: Agencia de Protección Ambiental from Buenos Aires, Secretaría de Ambiente from Córdoba, Comité Técnico Ejecutivo from Bahía Blanca, and Servicio Meteorológico Nacional for the meteorological data.

In order to evaluate the model performance concerning regional behavior, air quality satellite-based products are also used. NO_2 tropospheric column Level 2 product obtained by the OMI sensor (www.temis.nl, [48]) on board of the Aura platform (NASA) is compared to the CHIMERE NO_2 column. The OMI Level 2 was cloud screened removing pixels having a cloud fraction >40%. Uncertainties are described in [49] to be taking place mainly in the estimation of air mass factor due to presence and height of clouds, surface albedo, and vertical NO_2 profile. The CHIMERE model is sampled at the same time of OMI observations, and these are averaged over the model grid before comparison. If an OMI pixel falls in more than one model grid box, then the area fraction of the pixel overlapping each grid box is calculated and used as a weighting factor for the temporal average. The spatial correlation between the two fields (OMI and CHIMERE NO_2) is calculated for land, urban, and total domain pixels.

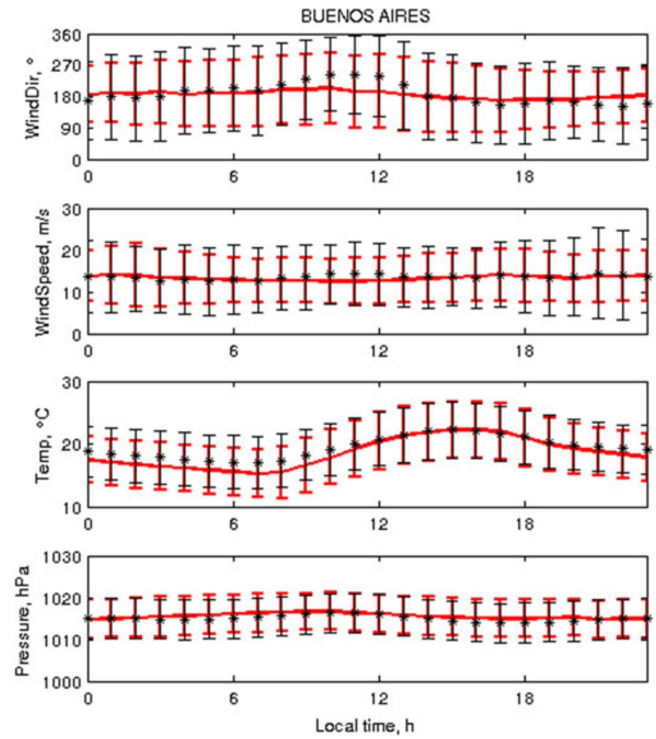

Fig. 5. Comparison of the observed (narrow black line) and simulated (bold red line) average daily cycle of meteorological variables near the ground in Buenos Aires (March–May 2009).

B. Modeling Evaluation

The chemical and meteorological variables evaluated correspond to those measured at different places in the country. Figs. 5–7 show hourly profiles of meteorological parameters estimated for the three-month period. At the same time, Figs. 8–10 show the same profiles for chemical variables. Table III presents statistical indexes obtained for each variable.

The daily cycle of the measured meteorological variables has characteristic profiles at each city, well simulated by the model. The statistical indexes indicate that the best meteorological variables simulated are temperature and pressure at every site, though Córdoba underestimates temperature for $2\,^{\circ}$C and pressure for 10 hPa. WRF has a very good performance with regard to wind speed, obtaining better simulations in Buenos Aires and Córdoba. Also, it can be noticed that WRF underestimates most of the meteorological variables in this three-month period, according to graphical and statistical analysis.

This article has been accepted for inclusion in a future issue of this journal. Content is final as presented, with the exception of pagination.

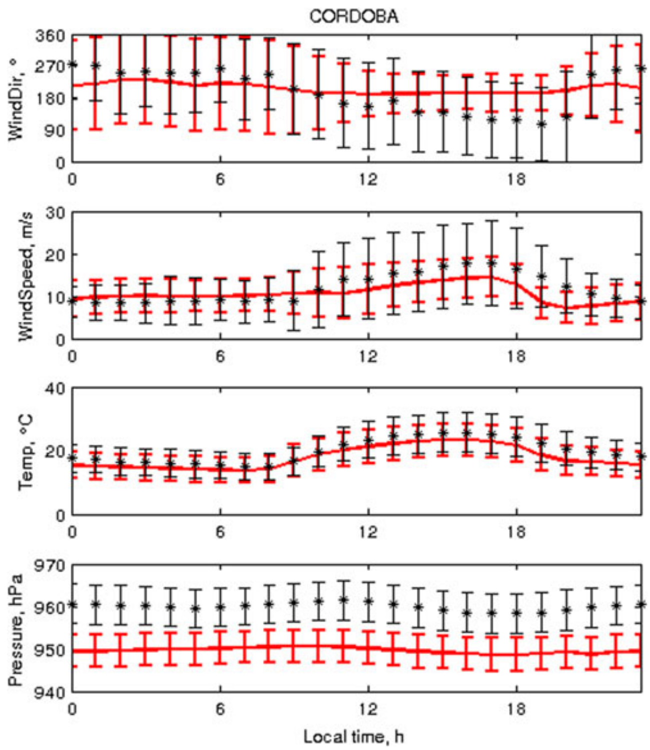

Fig. 6. Comparison of the observed (narrow black line) and simulated (bold red line) average daily cycle of meteorological variables near the ground in Córdoba (March–May 2009).

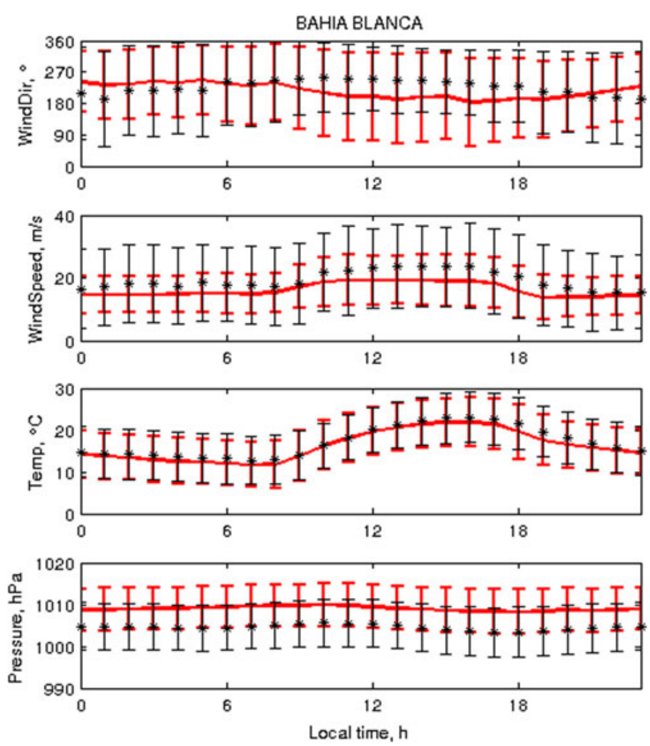

Fig. 7. Comparison of the observed (narrow black line) and simulated (bold red line) average daily cycle of meteorological variables near the ground in Bahía Blanca (March–May 2009).

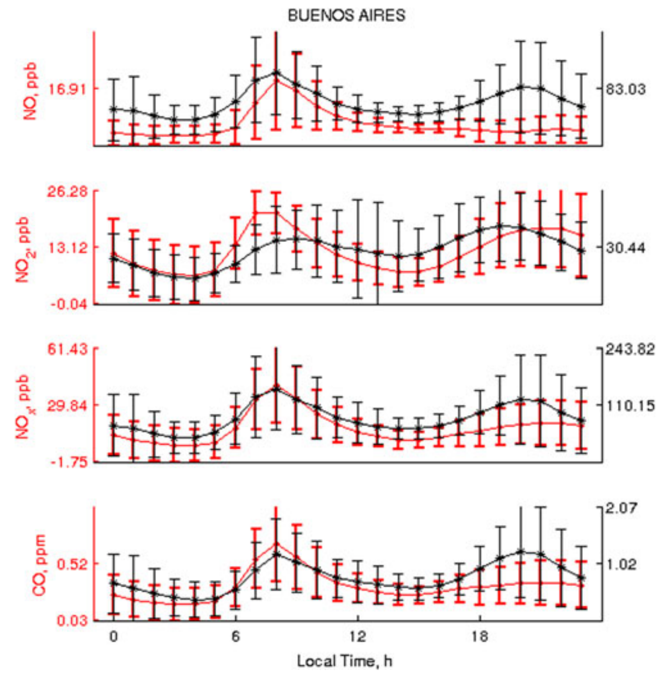

Fig. 8. Comparison of the observed (narrow black line) and simulated (bold red line) average daily cycle of chemical variables near the ground in Buenos Aires (March–May 2009).

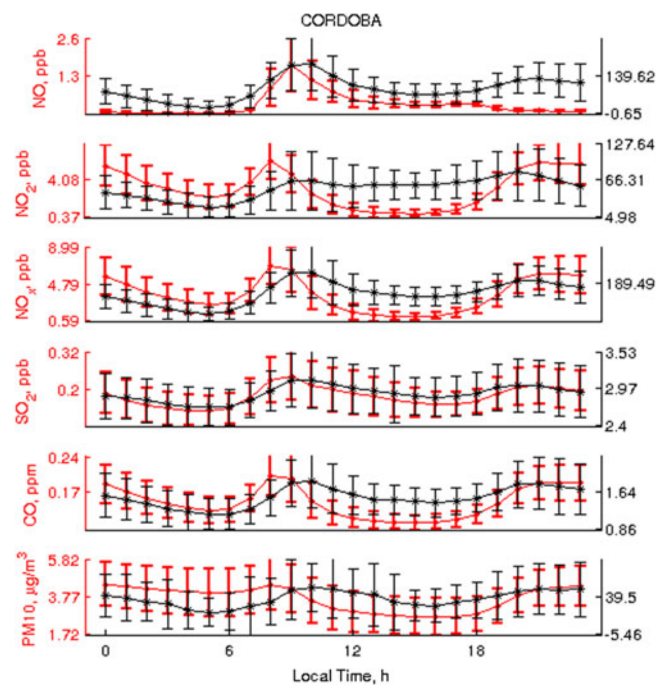

Fig. 9. Comparison of the observed (narrow black line) and simulated (bold red line) average daily cycle of chemical variables near the ground in Córdoba (March–May 2009).

In Buenos Aires, the estimated concentrations of pollutants are in the same magnitude order than the measured ones, mainly for NO_2 and CO. The monitoring site is identified as a high traffic place coherent with the hourly profile and observed concentrations of NO, higher than NO_2. At this resolution, we cannot expect to simulate well the traffic monitoring site.

This article has been accepted for inclusion in a future issue of this journal. Content is final as presented, with the exception of pagination.

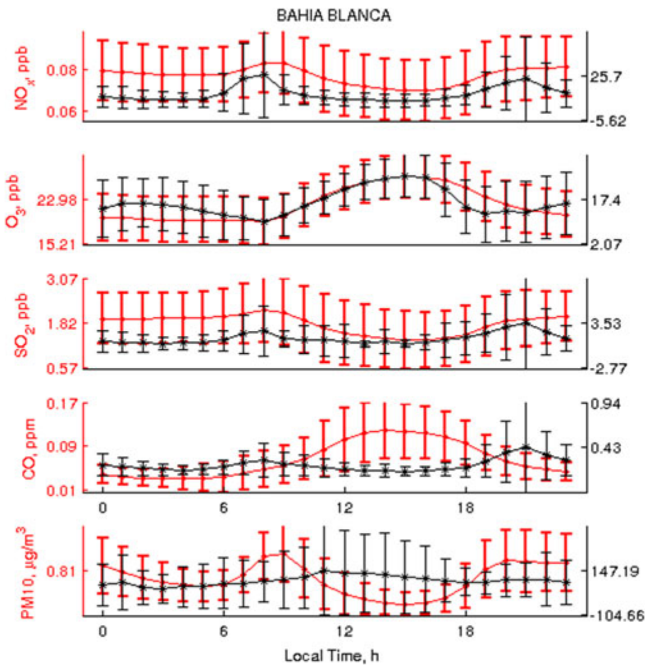

Fig. 10. Comparison of the observed (narrow black line) and simulated (bold red line) average daily cycle of chemical variables near the ground in Bahía Blanca (March–May 2009).

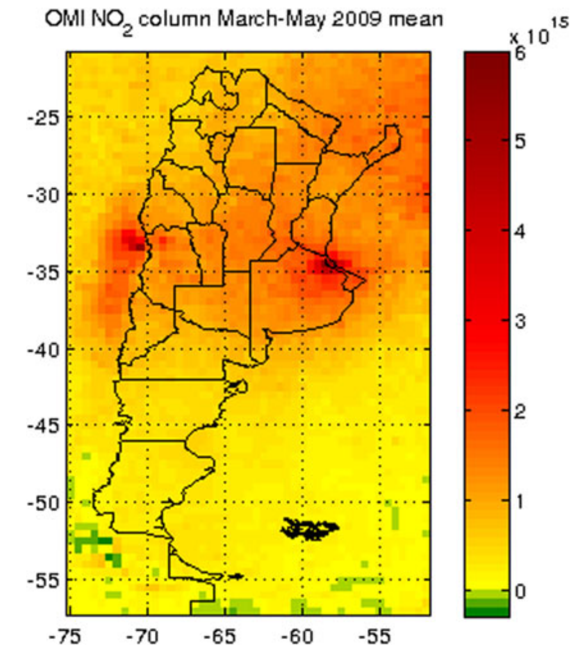

Fig. 11. March–May 2009 average NO_2 tropospheric column [molecules·cm^{-2}], obtained by the OMI sensor, on board the Aura satellite (NASA).

TABLE III
STATISTICAL INDICES OF THE COMPARISON BETWEEN OBSERVED AND SIMULATED CHEMICAL AND METEOROLOGICAL VARIABLES

Variable	bias	NMB, %	RMSE	r	Obs avg	Mod avg
			BUENOS AIRES			
T, °C	−0.84	−4.24	1.97	0.93	19.41	18.53
P, hPa	0.52	0.05	1.57	0.95	1014.94	1015.10
WS, km h^{-1}	−0.30	−2.21	6.72	0.58	13.49	13.26
WD, degrees	85.85	45.75	99.47	0.24	187.65	184.61
NO, ppb	−47.02	−91.50	71.42	0.50	51.39	4.57
NO_2, ppb	−16.65	−57.50	18.78	0.58	28.96	12.32
NO_x, ppb	−62.77	−79.00	83.38	0.66	79.45	16.89
CO, ppm	−0.43	−57.34	0.58	0.63	0.75	0.32
			CÓRDOBA			
T, °C	−2.10	−10.46	3.22	0.92	19.82	17.72
P, hPa	−10.35	−1.08	10.47	0.94	959.92	949.58
WS, km·h^{-1}	−1.39	−11.64	7.11	0.49	11.77	10.57
WD, degrees	83.80	41.73	98.74	0.21	200.80	206.14
NO, ppb	−90.14	−99.66	103.59	0.48	90.45	0.33
NO_2, ppb	−49.66	−94.03	55.88	0.07	52.81	3.20
NO_x, ppb	−140.07	−97.59	150.95	0.31	143.53	3.52
SO_2, ppb	−2.71	−93.80	2.69	0.15	2.89	0.18
CO, ppm	−1.38	−90.34	1.43	0.28	1.53	0.15
PM10, μg/m^3	−33.86	−90.07	42.58	−0.02	37.59	3.66
			BAHÍA BLANCA			
T, °C	−0.91	−5.16	2.29	0.96	17.07	16.17
P, hPa	4.45	0.44	4.69	0.96	1004.51	1008.99
WS, km·h^{-1}	−3.14	−16.15	10.38	0.63	19.21	16.18
WD, degrees	71.10	31.32	87.95	0.30	227.00	215.54
NO_x, ppb	−13.26	−99.43	17.83	0	13.34	0.08
SO_2, ppb	4.55	27.39	5.55	0.71	1.37	1.80
O_3, ppb	0.38	28.00	2.43	0.07	16.61	22.17
CO, ppm	−0.16	−70.23	0.22	−0.06	0.22	0.07
PM10, μg/m^3	−91.10	−99.27	152.93	−0.04	91.77	0.70

Additionally, the model underestimates the last peak emissions of NO. The simulated concentrations of NO_2 in the daily cycle do not show the same profile of the measurements, NO_2 reached, and overpassed NO concentrations. Further, simulated and measured CO are similar, though for the last hours, concentration peak of this species is also underestimated by CHIMERE.

In Córdoba and Bahía Blanca, the simulated concentrations are one or two orders of magnitude lower than the measurements. Most of the species follow the observed pattern, though for NO in Córdoba, the behavior is similar to that in Buenos Aires, and CO in Bahía Blanca has a nontraffic estimation profile.

Statistical indexes show an acceptable correlation between measured and simulated NO, NO_2, NO_x, and CO for Buenos Aires and SO_2 for Bahía Blanca, low correlation for NO and CO in Córdoba and no correlation between NO_2, PM10, and SO_2 for Córdoba, and NO_x, O_3, CO, and PM10 for Bahía Blanca. Moreover, the smaller differences obtained by NMB are for SO_2 and O_3 in Bahía Blanca, and NO_2 and CO in Buenos Aires. Córdoba has a very bad behavior when all the NMBs are evaluated.

Estimations and measurements of O_3 and SO_2, in Bahía Blanca, are of the same order and show similar profiles (see Fig. 10). Statistical indexes for these two species show correspondence, though O_3 is better estimated than SO_2. Whereas SO_2 has a lower RMSE, O_3 shows a smaller data dispersion. In both cases, the NMB is similar. It is important to say that O_3 concentrations do not differ from what background concentrations are expected to be.

Model evaluation was also performed against satellite data. NO_2 tropospheric column, obtained by the OMI sensor and

This article has been accepted for inclusion in a future issue of this journal. Content is final as presented, with the exception of pagination.

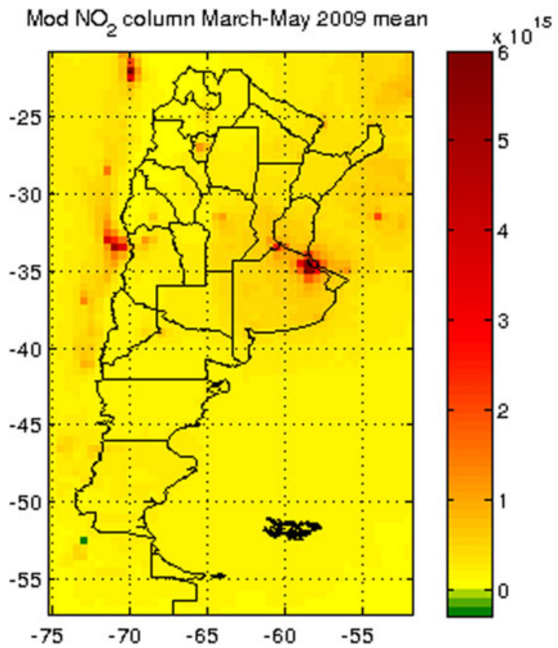

Fig. 12. March–May 2009 average NO_2 tropospheric column [molecules·cm^{-2}], obtained by the WRF-CHIMERE-EDGAR modeling system.

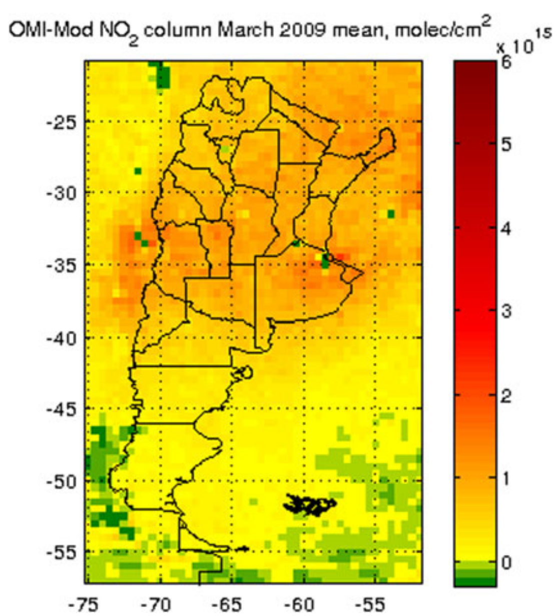

Fig. 13. NO_2 tropospheric column [molecules·cm^{-2}], bias (OMI—Model).

CHIMERE model, was averaged over the full three-month period (see Figs. 11 and 12). Differences between the two images are shown in Fig. 13. Regression plots for land, urban, and total domain pixels are shown in Fig. 14. Linear fitting parameters obtained are presented in Table IV, where $[NO_2]_{\rm CHIM}$ and $[NO_2]_{\rm OMI}$ are expressed in terms of tropospheric column, [molecules·cm^{-2}]. Bias over land class and total domain are similar; the low value of the fitting slope denotes a general underestimation of CHIMERE NO_2 column, although Fig. 13 illustrates that the model low bias takes place mostly over remote and unpolluted areas, whereas a model high bias can be seen

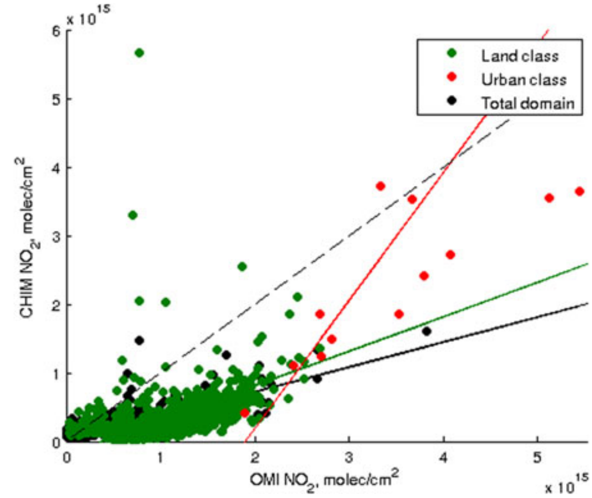

Fig. 14. NO_2 tropospheric column [molecules·cm^{-2}], CHIMERE versus OMI fitting curve for land class, urban class, and total spatial domain.

TABLE IV
NO_2 TOTAL COLUMN OMI VERSUS CHIMERE: LINEAR FITTING PARAMETERS

	a	b	R^2
land class	0.50	-1.87×10^{14}	0.36
urban class	1.87	-3.54×10^{15}	0.55
total domain	0.36	4.18×10^{11}	0.36

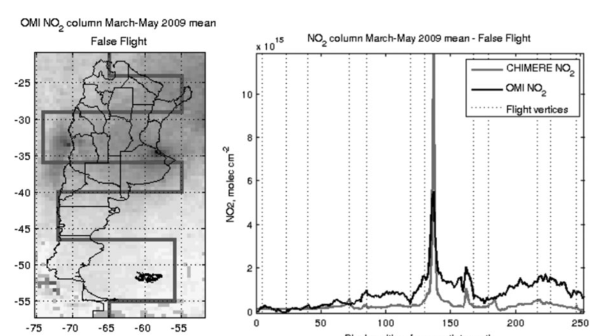

Fig. 15. Fake flight across the spatial domain (left) and NO_2 behavior for OMI and CHIMERE, during the "flight" (South to North direction, right). Vertices of the flight are also shown to help visualization of the results.

over Buenos Aires and Santiago de Chile megacities achieving the best correlation.

Additionally, Fig. 15 displays the behavior of the NO_2 column in a "fake flight" along the spatial domain, for the OMI and CHIMERE data. The model follows the OMI profile quite well, exhibiting underestimation from $-46°$ latitude toward north and overestimation near Buenos Aires. Santiago de Chile surroundings show a peak in both cases. Overall, OMI NO_2 tropospheric column spatial features are broadly captured by the model, whereas magnitudes are reproduced quite well over megacities, but underestimated over suburban and rural areas. This could be attributable to a too short simulated NO_2 lifetime. Indeed, Valin, Russell, Hudman, and Cohen [50] reported that dilution of NO_x emissions into coarse grid models tends to artificially shorted the NO_2 lifetime, because not enough OH suppression is taking place in the small-scale plumes into the model.

V. Conclusion and Future Work

This work presents the first implementation of a chemical transport model over the entire territory of Argentina. Performance of the WRF-EDGAR-CHIMERE modeling system has been evaluated using ground-based and satellite data.

In terms of emissions, Buenos Aires and Córdoba showed an urban characterization, and Bahía Blanca, which is an important petrochemical pole and port in the region, had an agricultural profile indicating missing information in the emission inventory. Additionally, previous studies point out that the concentration of PM10 in Córdoba is twice higher than in Buenos Aires when EDGAR emissions are one order lower roughly without traffic sources (see Figs. 2 and 3).

The WRF model outputs, which drove the CHIMERE simulations with meteorological variables, were shown to be robust within the period of time evaluated.

We found generally low correlation between observed and simulated values at Bahia Blanca and Córdoba; hourly profiles were fairly well followed by the simulations in the three cities (see Figs. 8–10). The reason this happened could not only be emissions, but the evident difference between a punctual measurement and a 3-D coarse resolution grid.

The evaluation of the model output with the NO_2 satellite product added more and better results. CHIMERE low bias occurs mostly over remote and unpolluted areas; model high bias can be seen over Buenos Aires and Santiago de Chile and the oceans. Moreover, OMI NO_2 tropospheric column spatial features are broadly captured by the model. This might be attributable to a too short simulated NO_2 lifetime [50].

From these results and previous works, it can be concluded that the implementation of this modeling system over Argentina could be improved by reviewing the emission inventory for the entire domain and continuing with the performance evaluation over longer periods of time, also considering satellite data of different sensors. Moreover, further development of the country air quality network, in terms of spatial coverage and representativeness would be highly desirable. The WRF-CHIMERE-EDGAR modeling system illustrated here already provides operational air quality forecast (http://meteo.caearte.conae.gov.ar).

Acknowledgment

M. F. García Ferreyra would like to thank CONAE and ASI particularly because of the scholarship awarded in the frame of AEARTE's Master program (National University of Córdoba) and M. Scavuzzo for his valuable personal guidance during the Master and afterwards.

References

[1] L. Menut *et al.*, "CHIMERE 2013: A model for regional atmospheric composition modelling," *Geosci. Model Develop.*, vol. 6, pp. 981–1028, 2013.

[2] L. E. Venegas and N. A. Mazzeo, "Modelling of urban background pollution in Buenos Aires City (Argentina)," *Environ. Model. Softw.*, vol. 21, pp. 577–586, 2006.

[3] H. Bogo, R. M. Negri, and E. San Román, "Continuous measurement of gaseous pollutants in Buenos Aires city," *Atmos. Environ.*, vol. 33, pp. 2587–2598, 1999.

[4] H. Bogo *et al.*, "Study of atmospheric particulate matter in Buenos Aires city," *Atmos. Environ.*, vol. 37, pp. 1135–1147, 2003.

[5] A. L. Pineda Rojas and L. E. Venegas, "Spatial distribution of ground-level background O3 concentrations in the Metropolitan Area of Buenos Aires, Argentna," *Environ. Pollution*, vol. 183, pp. 159–165, 2013.

[6] A. G. Ulke and N. Mazzeo, "Climatological aspects of the daytime mixing height in Buenos Aires city, Argentina," *Atmos. Environ.*, vol. 32, pp. 1615–1622, 1998.

[7] M. L. Bell, L. A. Cifuentes, L. D. Devra, E. Cushing, A. Gusman Telles, and N. Gouveia, "Environmental health indicators and a case study of air pollution in Latin American cities," *Environ. Res.*, vol. 111, pp. 57–66, 2011.

[8] A. E. Stein and B. M. Toselli, "Street level air pollution in Córdoba city, Argentina," *Atmos. Environ.*, vol. 30, pp. 3491–3495, 1996.

[9] M. L. López, S. Ceppi, G. G. Palancar, L. E. Olcese, G. Tirao, and B. M. Toselli, "Elemental concentration and source identification of PM10 and PM2.5 by SR-XRF in Córdoba City, Argentina," *Atmos. Environ.*, vol. 45, pp. 5450–5457, 2011.

[10] L. E. Olcese and B. M. Toselli, "Some aspects of air pollution in Córdoba, Argentina," *Atmos. Environ.*, vol. 36, pp. 299–306, 2002.

[11] H. A. Carreras, and M. L. Pignata, "Biomonitoring of heavy metals and air quality in Córdoba City, Argentina, using transplanted lichens." *Environ. Pollution*, vol. 117, pp. 77–87, 2002.

[12] H. A. Carreras, M. L. Pignata, and P. H. N. Saldiva, "In situ monitoring of urban air in Córdoba, Argentina using the Tradescantia-micronucleus (Trad-MCN) bioassay," *Atmos. Environ.*, vol. 40, pp. 7824–7830, 2006.

[13] E. Puliafito, M. Guevara, and C. Puliafito, "Characterization of urban air quality using GIS as a management system," *Environ. Pollution*, vol. 122, pp. 105–117, 2003.

[14] F. Norte, A. Ulke, S. Simonelli, and M. Viale, "The severe zonda wind event of 11 July 2006 east of the Andes Cordillera (argentine): A case study using the BRAMS model." *Meteorol. Atmos. Phys.*, vol. 102, pp. 1–14, 2008.

[15] S. E. Puliafito, D. G. Allende, C. G. Mulena, P. Cremades, and S. G. Lakkis, "Evaluation of the WRF model configuration for zonda wind events in a complex terrain," *Atmos. Res.*, vol. 166, pp. 24–32, 2015.

[16] U. Schlink *et al.*, "Ozone-monitoring in Mendoza, Argentina: Initial results," *J. Air Waste Manage.*, vol. 49, pp. 82–87, 1999.

[17] E. Puliafito and D. G. Allende, "Emission patterns of urban air pollution," *Revista Facultad de Ingeniería. Univ. Antioquia*, vol. 42, pp. 38–56, 2007.

[18] R. Fernández, D. Allende, F. Castro, P. Cremades, and E. Puliafito, "Regional air quality modeling using WRF/Chem: Implementation of global and local databases for Mendoza, Argentina," *Avances en Energías Renovables y Medio Ambiente*, vol. 14, pp. 43–50, 2010.

[19] G. Curci, "Origin of atmospheric aerosols at the Pierre Auger Observatory using studies of air mass trajectories in South America," *Atmos. Res.*, vol. 149, pp. 120–135, 2014.

[20] M. A. Orte, "Estudio y análisis de la contaminación atmosférica mediante técnicas físicas y químicas en los alrededores del Polo Petroquímico de La Plata," Master's thesis, Univ. Nacional del Centro de la Provincia de Buenos Aires, Tandil, Argentina, 2011.

[21] L. Massolo, M. Rehwagen, A. Porta, A. Ronco, O. Herbarth, and A. Mueller, "Indoor-outdoor distribution and risk assessment of volatile organic compounds in the atmosphere of industrial and urban areas," *Environ. Toxicol.*, vol. 25, pp. 339–349, 2010.

[22] F. Wichmann *et al.*, "Increased asthma and respiratory symptoms in childen exposed to petrochemical pollution," *J. Allergy Clin. Inmunol.*, vol. 123, pp. 632–638, 2009.

[23] N. Cianni *et al.*, "Calidad del aire y salud infantil en áreas urbanas e industriales de La Plata y Ensenada, Argentina," in *II Reunión arual Proyecto Integrador PROIMCA*. Buenos Aires, Argentina: Univ. Tecnol. Nacional, 2007.

[24] D. G. Allende, F. H. Castro, and S. E. Puliafito, "Air pollution characterization and modeling of an industrial intermediate city," *Int. J. Appl. Environ. Sci.*, vol. 5, pp. 275–296, 2010.

[25] V. R. Piriz-Carillo, N. I. Gasparri, H. R. Grau, and L. Paolini, "Monitoreo satelital de fuegos en el área cañera de la provincia de Tucumán, Argentina," *SELPER*, vol. 2, pp. 5–13, 2010.

[26] P. G. Cremades, D. G. Allende, and S. E. Puliafito, "Integración de modelos para la estimación del impacto en la calidad de aire de la quema de biomasa en el norte argentino," *Avances en Energías Renovables y Medio Ambiente*, vol. 15, pp. 37–44, 2011.

[27] A. Ipiña, G. M. Salum, E. Crinó, and R. D. Piacentini, "Satellite and ground detection of very dense smoke clouds produced on the islands of the Paraná river delta that affected a large region in Central Argentina," *Adv. Space Res.*, vol. 49, pp. 966–977, 2012.

[28] P. Cremades, D. Allende, and S. E. Puliafito, "Inventario de emisiones por quema de biomasa y estimación de su influencia en la calidad de aire en la Provincia de Tucumán," in *Contaminación Atmosférica e hídrica en Argentina. PROIMCA.* Buenos Aires, Argentina: Univ. Tecnol. Nacional, 2011.

[29] F. Castro-Videla, F. Barnaba, F. Angelini, P. Cremades, and G. P. Gobbi, "The relative role of Amazonian and non-Amazonian fires in building up the aerosol optical depth in South America: A five year study (2005-2009)," *Atmos. Res.*, vol. 122, pp. 298–309, 2013.

[30] EDGAR. Emission Database for Global Atmospheric Research (EDGAR), release version 4.0. European Commission, Joint Research Centre (JRC)/Netherlands Environmental Assessment Agency (PBL), 2009. [Online]. Available: http://edgar.jrc.ec.europa.eu

[31] W. C. Skamarock *et al.*, "A description of the Advanced Research WRF Version 2," NCAR, Boulder, CO, USA, Tech. Notes 468+STR, 2005.

[32] D. A. Hauglustaine *et al.*, "Interactive chemistry in the Laboratoire de Meteorologie Dynamique general circulation model: Description and background tropospheric chemistry evaluation." *J. Geophys. Res.*, vol. 109, p. D04314, 2004.

[33] P. Ginoux *et al.*, "Sources and distributions of dust aerosols simulated with the GOCART model," *J. Geophys. Res.*, vol. 106, pp. 20255–20273, 2001.

[34] M. Schultz *et al.*, "Radiative forcing by aerosols as derived from the AeroCom present-day and pre-industrial simulations," *Atmos. Chem. Phys.*, vol. 6, pp. 5225–5246, 2006.

[35] C. Textor *et al.*, "Analysis and quantification of the diversities of aerosol life cycles within AeroCom," *Atmos. Chem. Phys.*, vol. 6, pp. 1777–1813, 2006.

[36] F. Dentener *et al.*, "Emissions of primary aerosol and precursor gases in the years 2000 and 1750 prescribed data-sets for AeroCom," *Atmos. Chem. Phys.*, vol. 6, pp. 4321–4344, 2006.

[37] M. C. Hansen and B. Reed, "A comparison of the IGBP discover and University of Maryland 1 km global land cover products," *Int. J. Remote Sens.*, vol. 21, pp. 1365–1373, 2000.

[38] A. Guenther, T. Karl, P. Harley, C. Wiedinmyer, P. I. Palmer, and C. Geron, "Estimates of global terrestrial isoprene emissions using MEGAN (Model of Emissions of Gases and Aerosols from Nature)," *Atmos. Chem. Phys.*, vol. 6, pp. 3181–3210, 2006.

[39] National Centers for Environmental Prediction/National Weather Service/NOAA/U.S. Department of Commerce, "NCEP FNL operational model global tropospheric analyses, continuing from July 1999," Research Data Archive at the National Center for Atmospheric Research, Computational and Information Systems Laboratory, 2000. [Online]. Available: http://dx.doi.org/10.5065/D6M043C6

[40] H. Schmidt, C. Derognat, R. Vautard, and M. Beekmann, "A comparison of simulated and observed ozone mixing ratios for the summer of 1998 in Western Europe," *Atmos. Environ.*, vol. 35, pp. 6277–6297, 2001.

[41] J. J. Ruiz, C. Saulo, and J. Nogues-Paegle, "WRF model sensitivity to choice of parameterization over South America: Validation against surface variables," *Monthly Weather Rev.*, vol. 138, pp. 3342–3355, 2010.

[42] E. I. Society, *Generation of European Emission Data for Episodes (GENEMIS) Project, EUROTRAC Annual Report 1993, Part 5*. Garmisch-Partenkirchen, Germany: EUROTRAC, Garmish-Partenkirchen, 1994.

[43] Fundación Bariloche, "Inventario nacional de la República Argentina, de fuentes de emisiones y absorciones de gases de efecto invernadero, no controlados por el Protocolo de Montreal. Inventario correspondiente al año 2000 y revisión de los inventarios 1990, 194 y 1997," Secretaría de Ambiente de la Nación, San Martin, Argentina, 2005.

[44] S. E. Puliafito, D. Allende, S. Pinto, and P. Castesana, "High resolution inventory of GHG emissions of the road transport sector in argentina," *Atmos. Environ.*, vol. 101, pp. 303–311, 2015.

[45] R. Dennis *et al.*, "A framework for evaluating regional-scale numerical photochemical modeling systems," *Environ. Fluid Mech.*, vol. 10, pp. 471–489, 2010.

[46] P. Thunis, A. Pederzoli, and D. Pernigotti, "Performance criteria to evaluate air quality modeling applications," *Atmos. Environ.*, vol. 59, pp. 476–482, 2012.

[47] J. Swall and K. Foley, "The impact of spatial correlation and incommensurability on model evaluation," *Atmos. Environ.*, vol. 43, pp. 1204–1217, 2009.

[48] K. F. Boersma *et al.*, "An improved retrieval of tropospheric NO2 columns from the ozone monitoring instrument." *Atmos. Meas. Tech.*, vol. 4, pp. 1905–1928, 2011.

[49] K. F. Boersma, H. J. Eskes, and E. J. Brinksma, "Error analysis for tropospheric NO2 retrieval from space," *J. Geophys. Res.*, vol. 109, p. D04311, 2004.

[50] L. C. Valin, A. R. Russell, R. C. Hudman, and R. C. Cohen, "Effects of model resolution on the interpretation of satellite NO2 observations," *Atmos. Chem. Phys.*, vol. 11, pp. 11647–11655, 2011.

María Fernanda García Ferreyra was born in Córdoba, Argentina, on March 19, 1983. She received the degree in chemistry from the National University of Córdoba, Córdoba, in 2008, where she started working with air quality biomonitoring, and the master's degree in space applications for emergency early warning and response (AEARTE program), granted by the Argentinian and Italian Space Agencies (CONAE and ASI), allowing her to have a study stage in CETEMPS, L'Aquila, Italy, where she started developing the present work.

Since 2013, she has been with the CAEARTE Unity in CONAE, Falda del Canete, Argentina, where she generates satellite-based value-added products for environmental emergencies management and continues with air quality studies involving modeling and satellite monitoring.

Gabriele Curci was born in Rome, Italy, on October 14, 1977. He received the degree (*summa cum laude*) in 2002 and the Ph.D. in physics in 2006 from the University of L'Aquila, L'Aquila, Italy.

Since 2007, he has been a Researcher and Assistant Professor with the Department of Physical and Chemical Sciences, University of L'Aquila, where he is a Member of the Centre of Excellence on Weather Forecast (CETEMPS). He was a visiting student with Harvard University in 2001 and a Postdoctoral Fellow with the Laboratoire des Systémes Atmosphériques (LISA), Paris, France, in 2006–2007. His work focuses on the development and application of atmospheric composition models from the global to the local scale, with a particular focus on air quality forecast, integration with satellite observations, inversion of emissions sources, modeling of aerosol optical properties, and aerosol–cloud interactions.

Mario Lanfri received the B.Sc degree in physics in 1987 from the National University of Córdoba.

He was a Researcher and Teacher with the Atmospheric Physical Group, Faculty of Mathematics, Astronomy and Physics, National University of Córdoba (UNC), Córdoba, Argentina, from 1984 to 1997. Since 1997, he has been working with the Argentinian Space Agency (CONAE), Falda del Canete, Argentina. He cooperated in the ARGONAUTA Telemedicin Project. He worked in landscape epidemiology and the development of health applications from spatial information. He has been a Project Manager of the International Charter on Space and Major Disasters in several activations. He is currently a Professor with UNC, where he is in charge of the "Imagery digital processing and SIG" course of the AEARTE master in the Gulich Institute (CONAE-UNC). He supervises the CAEARTE Unity (Consultancy in Space Applications for Emergency Early Warning and Response) and responsible before environmental emergencies in Argentina, of the CONAE response.